

# Transition Matrix Computation and Reduction of Boundary Error Using Smooth Multiwavelet Bases

E.P. Sumesh and Elizabeth Elias

*National Institute of Technology,  
Calicut, India*

## Abstract

In this paper we discuss about a differential operator modeling using multiwavelets as a tool to solve partial differential equations (PDEs). It has been argued here that the advantages of smooth multiwavelets make them more suitable for solving PDEs by multiwavelet methods. Multiwavelet methods offer resolution at multilevels and higher approximation order in the boundary for a given filter length. Emphasis is given on calculation of a transition matrix for smooth multiwavelet bases. We propose a new multigrid method in conjunction with a transition matrix approach for solving PDEs to reduce the error near the boundary. The method is also applicable for any general boundary condition. Numerical results are discussed for a second-order PDE.

**Keywords:** Multiwavelets, transition matrix, difference operator, multigrid.

## 1. Introduction

Partial Differential Equations (PDEs) are powerful tools for modeling physical phenomena. Laplace's equation, Poisson's equation, Maxwell's equations, and diffusion equations are a few examples which find wide engineering applications. Solving PDEs using wavelets has drawn a lot of research in recent years. The methods used to solve PDEs are broadly divided into two types, algebraic methods and numerical methods. Algebraic methods are suitable when the solution has a closed algebraic form. Numerical methods are the most suitable when the solution does not have a closed form. Wavelets and multiwavelets are among the latest tools used to solve PDEs numerically [1, 2].

Solutions of PDEs using multiwavelets were developed by Alpert using Legendre type multiwavelets and it is proved that Legendre multiwavelets reduce the error to a level below that of scalar wavelets [3-5].

Legendre multiwavelets are a mutation of Haar's wavelet; they are piecewise linear and have short support, but they lack smoothness and are discontinuous. This leads to higher error when a continuous function is represented in a given space  $V_n^k$ , compared to those using smooth multiwavelets. Moreover Legendre multiwavelets are localized in time but not in frequency due to their discontinuity. Smooth multiwavelets have the advantage of being mostly simultaneously localized in time and frequency, of course within the limit imposed by Heisenberg's uncertainty principle.

Problems in semiconductor theory, electromagnetism and fluid dynamics have smooth solutions. Thus the use of smooth multiwavelet bases provides a better representation of these solutions. In this paper we use smooth multiwavelets to solve PDEs and propose a new approach for reducing the error near the boundary with the help of new grid points of smaller size.

The use of multiwavelets offers distinct advantage over scalar wavelet based systems, for which smoother the wavelet, longer the support needed. Multiwavelets avoid this difficulty by the use of a set of short support filters, yielding smoothness offered by wavelets with larger support, which leads to more compaction. In wavelets, symmetry is not possible unless we give up one of the other property like orthogonality. In multiwavelet bases, symmetry is possible without giving up orthogonality or other desirable properties. The linear phase symmetry property of multiwavelets improves the performance in the boundary, compared to scalar wavelets [6]. The interpolating property of multiwavelet bases, makes the coefficient values to be the same as the values of the solution, a unique property not satisfied by scalar wavelets.

Partial differential equations are often integro-differential equations. The requirements for differential and integral operators are contradictory which results in dense matrices, while modeling integral operators, when wavelet bases are used [3]. The use of multiwavelet bases leads to sparse representation for both of these operators. Wavelet and multiwavelet systems make the numerical calculus of operators practical, leading to exact linear part schemes for time discretisation of operators [1, 2, 7, 8]. Multiwavelets have the extra advantage of accommodating boundary condition without losing the order of approximation by virtue of their short support. A multiwavelet base with  $m$  vanishing moments maintains convergence of order  $m-1$ , up to the boundary. Boundary error due to large filter length is a major problem in any signal processing applications, including those using scalar wavelets. Multiwavelets provide a solution to this problem as they consist of a group of short filters spanning a given support. This reduces the error at the boundary while maintaining the order of approximation.

In summary, multiwavelets have the ability to offer specified approximation order near the boundary, apart from other advantages like real valued basis functions with compact support, orthogonality, linear phase and symmetry simultaneously. These properties bring a wider scope and advantages to multiwavelets, compared to scalar wavelets.

The use of operator modeling converts differential equations to algebraic equations in the transform domain. These algebraic equations are solved to obtain the solution in

the transform domain. An inverse transform gets the actual solution in the time or space domain. The methodology is illustrated by considering a simple first-order Ordinary Differential Equation(ODE) in the time domain as follows

$$\frac{du}{dt} = \sin \omega t \quad (1)$$

where  $\sin \omega t$  is the forcing function.

Taking multiwavelet transform of both sides of equation (1) yields

$$RU = F \quad (2)$$

where  $F$  is the multiwavelet transform of the forcing function and  $RU$  is that of  $\frac{du}{dt}$ .

$R$  is defined as the transition matrix used to model the differential operator and  $U$  is the multiwavelet transform of  $u$ . Equation (2) is easily solvable to obtain the solution  $U$ . The actual solution  $u$  is obtained by taking the inverse multiwavelet transform of  $U$ .

The same methodology applied to the ODEs is applied to solve PDEs also. We demonstrate this with an example

$$u_t = -x u_x, \quad x \in \Omega \in [0,1] \quad (3)$$

where

$$u = u(x,t) \in \mathbb{R}^n, \quad x \in [0,1] \quad \text{and} \quad t \in [0,1].$$

The initial conditions at  $t = 0$  is

$$u(x,0) = u_0(x) = x, \quad x \in \Omega \in [0,1], \quad (4)$$

and the boundary condition is

$$u(0,t) = 0, \quad t \in [0,1]. \quad (5)$$

The exact solution is  $u = xe^{-t}$ . We denote  $U(t_0)$  as the multiwavelet transform of the left-hand side of the equation (3) at  $t = 0$ . We make use of the initial conditions  $u(x,0)$ , together with the procedure used to solve the ODE to obtain the solution of (3) at  $t = 0$ . The solution  $u(x,t)$  is computed by discretising the time interval  $[0, 1]$  into  $N$  subintervals [3] of length  $\Delta t = 1/N$  and by repeatedly computing

$$U(t_{j+1}) = e^{-\Delta t} U(t_j), \quad \text{for } j = 0, 1, 2 \dots N-1. \quad (6)$$

Multiwavelets provide additional flexibility to incorporate boundary conditions in the operator modeling. The computation of the transition matrix is directly obtained for multiwavelet bases having closed form equations such as Legendre multiwavelets [9]. In this paper we propose a new method for computing the transition matrix in multiwavelet bases such as the DGHM multiwavelets which do not have a closed form representation. The method is a generalized one and can be directly applied to other types of multiwavelets as well. The use of smooth bases results in a reduction of

the error in representing differential operators, since the solution is not discontinuous in most of the natural phenomena. The variation of the transition matrix for different sampling frequencies is computed, which reduces the computational requirement. The error in the boundary is reduced by incorporating boundary conditions into the operator. A new method using multigrid near the boundary is employed to reduce the boundary error further.

This paper is organized as follows. A brief review of multiwavelet theory and operator modeling concepts is presented in section 2. The new general method of operator modeling is described in section 3 and the new proposed method of error reduction with a numerical example follows in section 4. Concluding remarks are stated in section 5.

## 2. Multiwavelet Bases and Differential operator Modeling

Multiwavelets with scaling function  $\Phi(t)$  and wavelet function  $\Psi(t)$  are given by

$$\Phi(t) = [\phi_1(t) \ \phi_2(t) \ \dots \ \phi_m(t)]^T \quad (7.1)$$

$$\Psi(t) = [\psi_1(t) \ \psi_2(t) \ \dots \ \psi_m(t)]^T \quad (7.2)$$

Figure 1 shows the scaling and wavelet functions for the Donovan, Geronimo, Hardin and Massopust (DGHM) multiwavelet system [10].

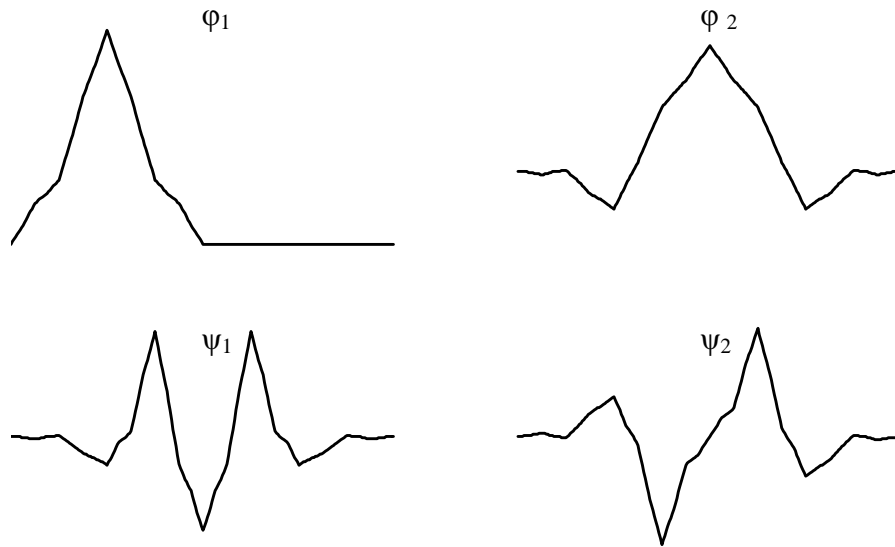


**Figure 1:** DGHM multiwavelet scaling function  $\phi_1$  and  $\phi_2$  and corresponding wavelet functions  $\psi_1$  and  $\psi_2$ .

The two-scale difference equations for multiwavelets are similar to those of the scalar wavelets.  $\Phi(t)$  and  $\Psi(t)$  can be expressed by the two-scale difference equations.

$$\Phi(t) = \sqrt{2} \sum_{m=-\infty}^{\infty} H_m \Phi(2t - m) \quad (8.1)$$

$$\Psi(t) = \sqrt{2} \sum_{m=-\infty}^{\infty} G_m \Phi(2t - m) \quad (8.2)$$

where  $H_m$  and  $G_m$  are  $k \times k$  matrix filters.

Using fractal interpolation, Geronimo, Hardin and Massopust [10] constructed GHM multiwavelet functions with  $k = 2$ . The matrix filters  $H_m$  and  $G_m$  are given for  $m = 0, 1, 2$  and  $3$ .

$$H_0 = \sqrt{2} \begin{bmatrix} 3/10 & 2\sqrt{2}/5 \\ -\sqrt{2}/40 & -3/20 \end{bmatrix} \quad (9.1)$$

$$H_1 = \sqrt{2} \begin{bmatrix} 3/10 & 0 \\ -9\sqrt{2}/40 & 1/2 \end{bmatrix} \quad (9.2)$$

$$H_2 = \sqrt{2} \begin{bmatrix} 0 & 0 \\ -\sqrt{2}/40 & -3/20 \end{bmatrix} \quad (9.3)$$

$$H_3 = \sqrt{2} \begin{bmatrix} 0 & 0 \\ -\sqrt{2}/40 & 0 \end{bmatrix} \quad (9.4)$$

$$G_0 = \sqrt{2} \begin{bmatrix} -\sqrt{2}/40 & -3/20 \\ -1/20 & -3\sqrt{2}/20 \end{bmatrix} \quad (10.1)$$

$$G_1 = \sqrt{2} \begin{bmatrix} 9\sqrt{2}/40 & -1/2 \\ 9/20 & 0 \end{bmatrix} \quad (10.2)$$

$$G_2 = \sqrt{2} \begin{bmatrix} 9\sqrt{2}/40 & -3/20 \\ -9/20 & 3\sqrt{2}/20 \end{bmatrix} \quad (10.3)$$

$$G_3 = \sqrt{2} \begin{bmatrix} -\sqrt{2}/40 & 0 \\ 1/20 & 0 \end{bmatrix} \quad (10.4)$$

The two-scale difference equations (8.1) and (8.2) show that the  $k \times k$  matrix low pass filter  $H_m$  and the  $k \times k$  matrix high pass filter  $G_m$  require an input of vectors during the convolution step. This needs a prefiltering step to convert the input data samples to vectors of size  $k$ . Interpolating prefilters, quadrature based prefilters, and Hardin-Roach prefilters [11, 12] are prefilter types that can be used with multiwavelet bases.

In summary, the data samples need prefiltering before they be given as input to a multiwavelet transformation step. The use of prefilter minimizes the energy compaction ratio of the multiwavelet coefficients. The energy compaction ratio is defined as the total energy of the output from high pass portions of the analysis filter bank divided by the total energy of the input signal [13]. Thus smaller the ratio, better the energy compaction.

Due to the preprocessing step, a postprocessing is required after taking the inverse multiwavelet transform for the reverse process of converting the vectors back to scalar. The use of balanced multiwavelets, eliminates the need of prefiltering and postprocessing steps [14, 15].

## 2.1 Modeling the Operator $d/dx$ in Multiwavelet Bases

A function  $f \in C^\infty([0,1])$  can be approximated by  $P_n^k f$  and its derivative by  $T_n^k f$  in the space  $V_n^k$  by a multiwavelet expansion [16, 17].

$(P_n^k f)(x)$  is defined as

$$(P_n^k f)(x) = \sum_{l=0}^{2^n-1} \sum_{j=0}^{k-1} S_{jl}^n \phi_{jl}^n(x) \quad (11)$$

where  $S_{jm}^n$  represents the multiwavelet expansion coefficients of  $f(x)$  in the space  $V_n^k$  [12]:

$$S_{jl}^n = \int_{2^{-n}l}^{2^{-n}(l+1)} f(x) \phi_{jl}^n(x) dx \quad (12)$$

In multiwavelet bases, a weak representation of the derivative operator is possible which makes it easy to apply boundary conditions without losing the approximation order.

Let  $(T_n^k f)(x)$  be the approximation of  $df(x)/dx$  in the space  $V_n^k$

$$(T_n^k f)(x) = \sum_{l=0}^{2^n-1} \sum_{j=0}^{k-1} \tilde{S}_{il}^n \phi_{il}^n(x) \quad (13)$$

where the coefficients  $\tilde{S}_{il}^n$  represent the multiwavelet expansion coefficients of  $df(x)/dx$  in the space  $V_n^k$ :

$$\tilde{S}_{il}^n = \int_{2^{-n}l}^{2^{-n}(l+1)} (df(x)/dx) \phi_{il}^n(x) dx. \quad (14)$$

Using (12) and (14) the  $k \times k$  transition matrix  $\begin{bmatrix} r_{lm}^n \end{bmatrix}$  is defined to satisfy

$$\tilde{S}_{il}^n = \sum_{m=0}^{2^n-1} \sum_{j=0}^{k-1} \begin{bmatrix} r_{lm}^n \end{bmatrix}_{ij} S_{jm}^n \quad (15)$$

where  $l, m = 0, 1, 2, \dots, 2^n - 1$ ,

$$\text{and } [r_{lm}^n]_{ij} = \int_{2^{-n}l}^{2^{-n}(l+1)} \phi_{il}^n(x) (d/dx) \phi_{jm}^n(x) dx. \quad (16)$$

We use the two-scale difference equations (8.1) and (8.2) to compute  $[r_{lm}^n]_{ij}$  from the  $k \times k$  transition matrix representation of the differential operator  $(d/dx)$  on the coarsest scale  $V_0^k$ .

$$[r_{lm}^n]_{ij} = 2^{nd} [r_{l-m}]_{ij} \quad (17)$$

where  $d$  is the order of approximation, and

$$[r_l]_{ij} = \int_0^s \phi_i(x) (d/dx) \phi_j(x+l) dx. \quad (18)$$

The  $k \times k$  transition matrix  $[r_l]_{ij}$  is the representation of  $(d/dx)$  on the coarsest scale  $V_0^k$  and  $[0, s]$  is the support of  $\Phi(x)$ .

For DGHM multiwavelets with  $k = 2$ , the value of  $d$  is unity.

Since  $d/dx$  is a local operator,  $r_l = 0$  for all values  $|l| > 1$ .

$$\text{Thus } \tilde{S}_{il}^n = 2^n \sum_{j=0}^{k-1} ([r_1]_{ij} S_{j,l-1}^n + [r_0]_{ij} S_{jl}^n + [r_{-1}]_{ij} S_{j,l+1}^n). \quad (19)$$

Equation (19) suggests that  $d/dx$  operator modeling is the computation of block stencils  $[r_1], [r_0]$  and  $[r_{-1}]$  [3, 9].

### 3. Computation of Transition Matrix for DGHM Multiwavelets

#### A Case Study

A very natural approach to generalize the differential operator modeling using smooth multiwavelet bases is to use DGHM multiwavelet with  $k = 2$ . A function  $f$  can be represented in the space  $V_n^k$  with the expansion coefficients  $S_{jm}^n$  and  $df(x)/dx$  by  $\tilde{S}_{il}^n$

$$[S_{jm}^n] = \begin{bmatrix} S_{0,0} & S_{0,1} & S_{0,2} & \cdots & S_{0,2^n-1} \\ S_{1,0} & S_{1,1} & S_{1,1} & \cdots & S_{1,2^n-1} \end{bmatrix} \quad (20)$$

$$[\tilde{S}_{jm}^n] = \begin{bmatrix} \tilde{S}_{0,0} & \tilde{S}_{0,1} & \tilde{S}_{0,2} & \cdots & \tilde{S}_{0,2^n-1} \\ \tilde{S}_{1,0} & \tilde{S}_{1,1} & \tilde{S}_{1,1} & \cdots & \tilde{S}_{1,2^n-1} \end{bmatrix} \quad (21)$$

In matrix form,  $S_{jm}^n$  and  $\tilde{S}_{il}^n$  are related by

$$[\tilde{S}_{jm}^n] = R^n [S_{jm}^n] \quad (22)$$

For the central difference operator  $D_C$ , the matrix  $R^n$  [18] can be expressed as

$$R^n = \begin{bmatrix} r_0 & r_{-1} & 0 & 0 & 0 & 0 & 0 & \cdots & 0 \\ r_1 & r_0 & r_{-1} & 0 & 0 & 0 & 0 & \cdots & 0 \\ 0 & r_1 & r_0 & r_{-1} & 0 & 0 & 0 & \cdots & 0 \\ \cdot & \cdot & \cdot & & & & \cdot & \cdot & \cdot \\ \cdot & \cdot & \cdot & & & & \cdot & \cdot & \cdot \\ 0 & 0 & 0 & 0 & \cdots & r_1 & r_0 & r_{-1} \\ 0 & 0 & 0 & 0 & \cdots & 0 & r_1 & r_0 \end{bmatrix} \quad (23)$$

where  $r_0 = \begin{bmatrix} r_{000} & r_{001} \\ r_{010} & r_{011} \end{bmatrix}$ ,  $r_{-1} = \begin{bmatrix} r_{-100} & r_{-101} \\ r_{-110} & r_{-111} \end{bmatrix}$  and  $r_1 = \begin{bmatrix} r_{100} & r_{101} \\ r_{110} & r_{111} \end{bmatrix}$ .

### 3.1 Computation of the Central Difference Operator

We propose a simple and direct method to compute  $r_0$ ,  $r_1$  and  $r_{-1}$ .

Equation (19) can be expanded for an arbitrary value of  $l$  where  $1 < l < 2^n - 2$ :

$$\tilde{S}_{ol} = 2^n \left[ [r_1]_{00} S_{0,l-1} + [r_1]_{01} S_{1,l-1} + [r_0]_{00} S_{0,l} + [r_0]_{01} S_{1,l} + [r_{-1}]_{00} S_{0,l+1} + [r_{-1}]_{01} S_{1,l+1} \right] \quad (24)$$

$$\tilde{S}_{il} = 2^n \left[ [r_1]_{10} S_{0,l-1} + [r_1]_{11} S_{1,l-1} + [r_0]_{10} S_{0,l} + [r_0]_{11} S_{1,l} + [r_{-1}]_{10} S_{0,l+1} + [r_{-1}]_{11} S_{1,l+1} \right] \quad (25)$$

In matrix form, equations (24) and (25) can be represented as

$$\begin{bmatrix} \tilde{S}_{ol} \\ \tilde{S}_{il} \end{bmatrix} = 2^n \begin{bmatrix} r_{100} & r_{101} & r_{000} & r_{001} & r_{-100} & r_{-101} \\ r_{110} & r_{111} & r_{010} & r_{011} & r_{-110} & r_{-111} \end{bmatrix} \begin{bmatrix} S_{0,l-1} & S_{1,l-1} & S_{0,l} & S_{1,l} & S_{0,l+1} & S_{1,l+1} \end{bmatrix}^T \quad (26)$$

The transition matrix is defined by the integral [9]

$$[r_l]_{ij} = \int_{2^{-n}l}^{2^{-n}(l+1)} d/dx \varphi_j(x+l) \cdot \varphi_i(x) dx \quad (27)$$

Note that in equation (27),  $[r_l]_{ij}$  depends only on the basis functions, and is independent of the signal. This fact is employed to compute  $[r_l]_{ij}$ . Multiwavelet coefficients of a smooth function  $f(x)$  (may be a sinusoidal signal represented in space  $V_n^k$ ) is computed to obtain  $S_{jm}^n$ . The multiwavelet coefficients of  $df(x)/dx$  will yield  $\tilde{S}_{il}^n$ . We use  $S_{jm}^n$  and  $\tilde{S}_{il}^n$  in (26), to obtain the block stencils  $[r_0]$ ,  $[r_{-1}]$  and  $[r_1]$  [18, 19]. Care must be taken while selecting  $l$  value in (26) so that the function or its derivative does not have any discontinuity or singularity near  $l$ , as one needs higher resolution space for their complete representation.

### 3.2 Computation of the Backward Difference Operator

Backward difference operators also can be used to model using

$$\tilde{S}_{il}^n = D_b S_{jm}^n \quad (28)$$

$$\text{where } D_b = \begin{bmatrix} r_0^c & 0 & 0 & 0 & 0 & 0 & 0 & \cdots & 0 \\ r_1 & r_0 & 0 & 0 & 0 & 0 & 0 & \cdots & 0 \\ 0 & r_1 & r_0 & 0 & 0 & 0 & 0 & \cdots & 0 \\ \cdot & \cdot & \cdot & & & & \cdot & \cdot & \cdot \\ \cdot & \cdot & \cdot & & & & \cdot & \cdot & \cdot \\ 0 & 0 & 0 & 0 & \cdots & r_1 & r_0 & 0 \\ 0 & 0 & 0 & 0 & \cdots & 0 & r_1 & r_0 \end{bmatrix} \quad (29)$$

and  $r_0^c$  is the corrected stencil near the left boundary to reduce boundary error.

Multiplication of the first row of  $D_b$  with the first column of  $S_{jm}^n$  gives

$$\begin{bmatrix} \tilde{S}_{00} \\ \tilde{S}_{10} \end{bmatrix} = \begin{bmatrix} r_0^c \\ r_1 \end{bmatrix} \begin{bmatrix} S_{00} \\ S_{10} \end{bmatrix} \quad (30)$$

$$\text{or } \tilde{S}_{00} = \begin{bmatrix} r_{000}^c & r_{001}^c \end{bmatrix} \begin{bmatrix} S_{00} \\ S_{10} \end{bmatrix} \text{ and } \tilde{S}_{10} = \begin{bmatrix} r_{010}^c & r_{011}^c \end{bmatrix} \begin{bmatrix} S_{00} \\ S_{10} \end{bmatrix} \quad (31)$$

Equation (31) can be solved to obtain  $r_0^c$  as described in section 3.1, by generating  $\tilde{S}_{il}^n$  and  $S_{jm}^n$  for two different signals satisfying the requirements given in section 3.1.

For any value of  $l$ ,  $0 < l < 2^n - 1$ , using (28) and (29) we obtain

$$\begin{bmatrix} \tilde{S}_{0l} \\ \tilde{S}_{1l} \end{bmatrix} = \begin{bmatrix} r_1 \\ r_0 \end{bmatrix} S_{l-1} + \begin{bmatrix} r_0 \\ r_1 \end{bmatrix} S_l \quad (32)$$

Equation (32) yields two linear equations:

$$\tilde{S}_{0l} = r_{111} S_{0,l-1} + r_{112} S_{1,l-1} + r_{011} S_{0,l} + r_{012} S_{1,l} \quad (33)$$

$$\tilde{S}_{1l} = r_{121} S_{0,l-1} + r_{122} S_{1,l-1} + r_{021} S_{0,l} + r_{022} S_{1,l} \quad (34)$$

The matrices  $r_0$  and  $r_1$  are obtained by solving (33) and (34)

Table 1 shows the values obtained for  $r_0^c$ ,  $r_0$  and  $r_1$  using DGHM multiwavelets.

**Table 1:** Block stencils of the transition matrices for first-order derivative using  $D_b$  (DGHM multiwavelet and Hardin-Roach prefilter with approximation order2 (ap2) [12, 13], for  $k=2$ )

$r_0^c$	$r_0$	$r_1$
$\begin{bmatrix} -2 & 2\sqrt{2} \\ -\sqrt{2} & 2 \end{bmatrix}$	$\begin{bmatrix} 2\sqrt{2} & -0.58774 \\ 2 & -0.38115 \end{bmatrix}$	$\begin{bmatrix} 0 & -3.4251 \\ 0 & -2.388 \end{bmatrix}$

The block stencils can be computed directly for the subspace  $V_n^k$  by multiplying  $r_0^c, r_0$  and  $r_1$  by the factor  $2^{nd}$  where  $d$  is the degree of homogeneity of the operator.

A similar method can be used for forward difference operators to model  $d/dx$  using multiwavelets to satisfy the following relation (35)

$$\tilde{S}_{il}^n = D_f S_{jm}^n \quad (35)$$

$$\text{where } D_f = \begin{bmatrix} r_0^l & r_{-1}^l & 0 & 0 & 0 & 0 & 0 \cdots 0 \\ 0 & r_0 & r_{-1} & 0 & 0 & 0 & 0 \cdots 0 \\ 0 & 0 & r_0 & r_{-1} & 0 & 0 & 0 \cdots 0 \\ \cdot & \cdot & \cdot & & & \cdot & \cdot & \cdot \\ \cdot & \cdot & \cdot & & & \cdot & \cdot & \cdot \\ 0 & 0 & 0 & 0 & \cdots & 0 & r_0 & r_{-1} \\ 0 & 0 & 0 & 0 & \cdots & 0 & 0 & r_0^r \end{bmatrix} \quad (36)$$

A similar procedure for computing  $D_b$  is used to obtain  $D_f$ .

The method described in section 3 can be employed for other types of multiwavelets with corresponding prefilters and also for balanced multiwavelets.

#### 4. Reduction of the Error in Boundaries

The reduction of the boundary error is illustrated using the PDE

$$u_t = (1/(\pi^2 - 1))u_{xx}, \quad x, t \in \Omega \in [0,1] \quad (37)$$

where  $u = u(x, t) \in R^n$ ,  $x \in [0,1]$  and  $t \in [0,1]$ .

The initial conditions are

$$u(x,0) = u_0(x) = \sin(\pi x), \quad (38)$$

and the boundary conditions are

$$u(0,t) = u(1,t) = 0. \quad (39)$$

$$\text{The exact solution is } u = e^{-(\pi^2/(\pi^2-1))t} \sin(\pi x). \quad (40)$$

The solution obtained by using the transition matrix approach described in section 3 at time  $t = 0.15608$  and  $0.9002$  is shown in Figure 2. The transition matrix shown in Table 1 is used to solve the equation (37), to obtain the solution for  $x, t \in [0,1]$  with  $2^n$  sample points.

The algorithm for obtaining the solution is as follows. The right-hand side of equation (37) can be expressed in terms of multiwavelet expansion coefficients in the space  $V_n^k$ .

We denote the multiwavelet transform (with necessary prefiltering) of  $x$  as  $\text{MWT}\{x\}$  and use equation (22)

$$\text{MWT}\{u_{xx}\} = \mathbf{R}[\mathbf{R}U] = \mathbf{R}^2[U] \quad (41)$$

where  $\mathbf{R}U$  is the MWT  $\{u_x\}$  and  $\mathbf{R}[\mathbf{R}U]$  or  $\mathbf{R}^2[U]$  is defined as the MWT  $\{u_{xx}\}$ . The error in modeling the second order derivative can be reduced by using the relation

$$R^2U = (D_b^T D_b + D_f^T D_f) / 2 \quad (42)$$

Equation (37) can be represented in the multiwavelet transform domain, with the use of (41) at time  $t_0 = 0$  as

$$U(t_0) = (1/(\pi^2 - 1))R^2U(x,0) \quad (43)$$

where  $U(x,0)$  in the MWT  $\{u(x,0)\}$ .

We use the equation (43) to compute  $U(t_0)$  at  $t = 0$ . The values of  $U(t_1)$  at time  $t_1 = \Delta t$  is obtained by the use of (6)

$$U(t_1) = e^{-(\pi^2/(\pi^2-1))\Delta t} U(t_0) \quad (44)$$

The value of  $U(t_1)$  can be used to solve the equation

$$U(t_1) = (1/(\pi^2 - 1))R^2U(x,t_1) \quad (45)$$

to obtain the new value of  $U(x,t_1)$ . The inverse multiwavelet transform of  $U(x,t_1)$ , followed by the necessary postfiltering, gives solution at the  $2^n$  sample points  $u(x,t_1)$ .

The procedure is repeated to obtain the values of  $u$  for the time  $t_2 = 2\Delta t$ ,  $t_3 = 3\Delta t, \dots, t_{N-1} = (N-1)\Delta t$ .

The obtained result is compared with the actual solution and the error is computed and is shown in Figure 3. Using Figures 2 and 3, it is inferred that the six left-most samples and six right-most samples are giving a boundary error even after using the corrected stencil  $r_0^c$  at the boundaries.

The error in the boundary has a maximum value of 0.1605 at time  $t = 0.9002$ , whereas that at the interior points is  $1 \times 10^{-5}$ . The maximum error at the interior points, if we use the same algorithms with Legendre multiwavelets, is of the order of  $10^{-3}$ . This indicates the advantage of smooth basis functions. The error at these six points near the left and right boundary at time  $t = 0.9002$  can be further reduced by using an algorithm using new grid as follows.

**Step 1.** The initial condition  $u(x,0) = u_0(x) = \sin(\pi x)$  is approximated in the space  $V_{n+1}^k$  by taking the multiwavelet transform. We use the multiwavelet coefficients obtained in equation (15) to compute the values of  $U(t_0)$ .

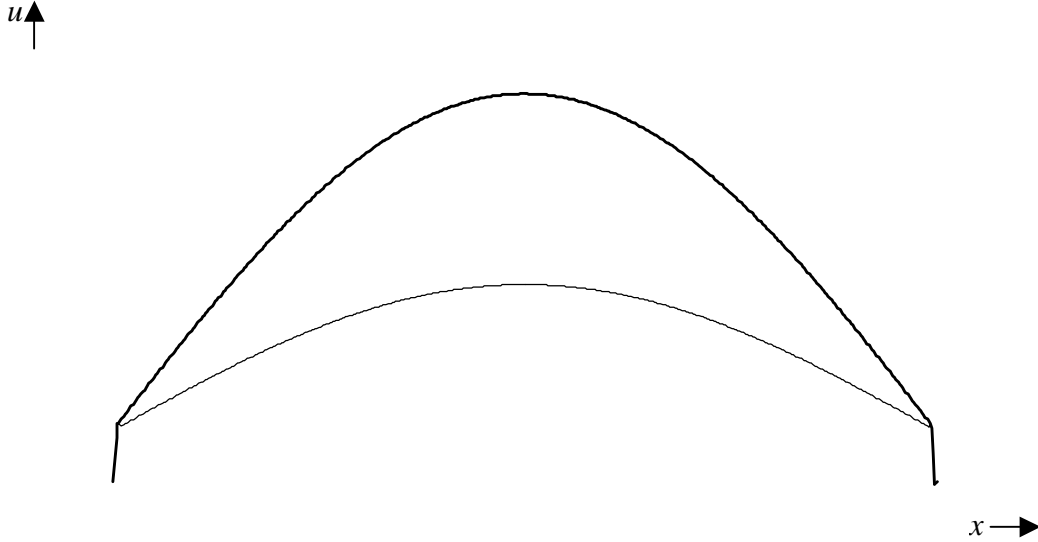


**Figure 2:** Solution of the PDE  $u_t = (1/(\pi^2 - 1))u_{xx}$  obtained using the transition matrix (DGHM Multiwavelet with ap2 prefilter type) at time  $t = 0.15608$  and  $0.9002$ .

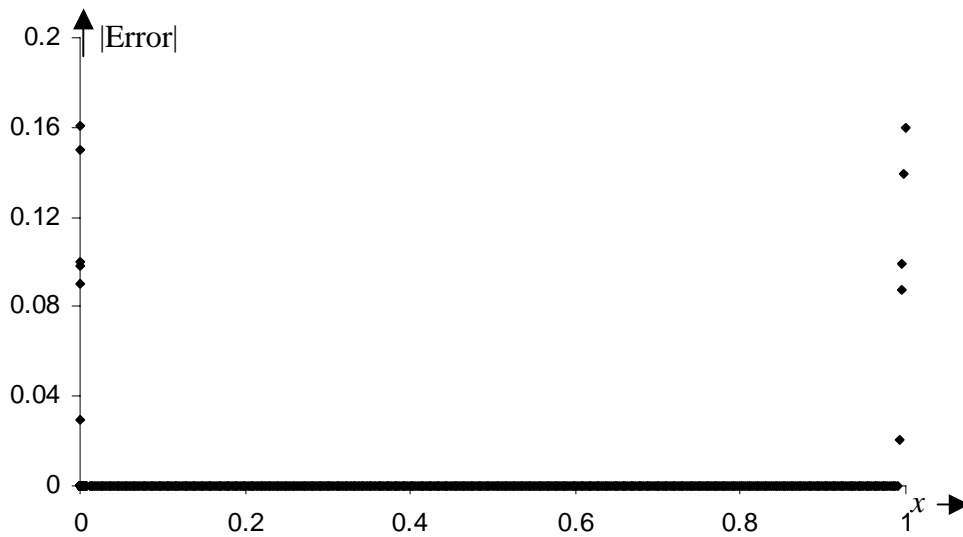


**Figure 3:** Magnitude of the error in the solution of the PDE  $u_t = (1/(\pi^2 - 1))u_{xx}$  obtained at time  $t = 0.9002$  using the transition matrix (DGHM multiwavelet with ap2 prefilter type).

**Step 2.** The values of  $U(t_0)$  obtained in *step 1* is used to compute the solution  $u(x,t)$  with a new grid size of  $1/2^{n+1}$  by a similar procedure discussed in section 4. The new

boundary conditions are  $u(0,0.9002) = 0$  in the left and that on right is the value of  $u(x,0.9002)$  obtained at  $x = 7/2^n$  and  $t = 0.9002$  in the space  $V_n^k$ . The right boundary of the new grid will still produce an error but the calculation for  $x > 5/2^n$  need not be done again because the solution is already obtained from the first grid itself. This reduces the extra computation required.

The steps 1 and 2 can be repeated again by reducing the grid by a factor of 2 each time, with the proper boundary conditions until a desired error tolerance or maximum resolution needed for  $x$  is met. A similar procedure is applied to the right boundary as well.

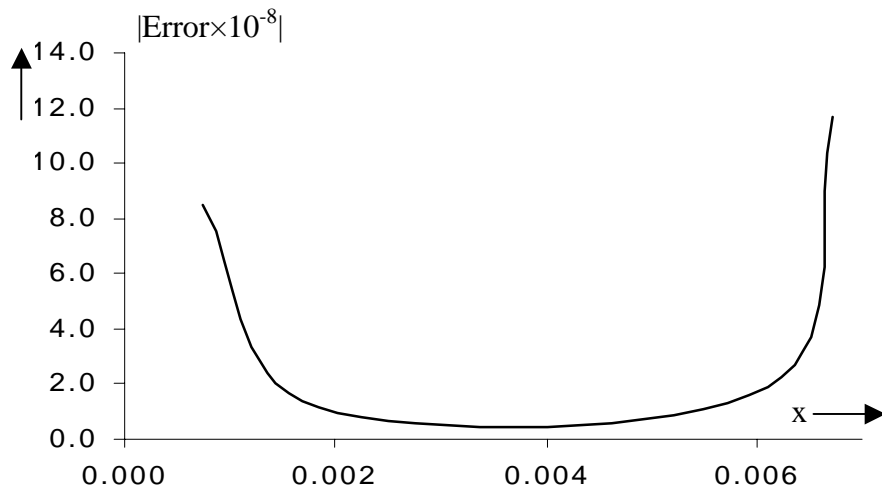


**Figure 4:** Magnitude of the error in the solution of the PDE  $u_t = (1/(\pi^2 - 1))u_{xx}$  obtained at time  $t = 0.9002$  using the transition matrix (DGHM multiwavelet with ap2 prefilter type) near the left boundary for the first multigrid with a grid size  $1/4$  of the actual size.

The same algorithm can be used if the grid size is reduced by a factor of  $2^p$  instead of 2, where  $p$  is an integer. Figure 4 shows the error in the left boundary using a multigrid of size  $1/2^{n+2}$ . It may be noted that the error for  $6/2^{n+2}$  to  $5/2^n$  is reduced to a maximum of  $8.5 \times 10^{-8}$ . The process of introducing new grids on the left boundary may be done until the boundary error is below the maximum permissible limit or a maximum resolution in  $x$  is reached.

A similar procedure can be done at the right boundary also until the error is below the maximum error permitted or a maximum resolution in  $x$  is reached. Figure 5 shows the error in the left boundary for a multigrid of size  $1/2^{n+4}$ . It may be noted that the error for  $6/2^{n+4}$  to  $5/2^{n+2}$  is reduced to a maximum of  $6.1 \times 10^{-10}$ .

Figure 6 shows that by reducing the size of the grid by a factor of 4 near the boundaries only after two iterations the error near the boundaries has reduced to a value even less than that of the interior points.

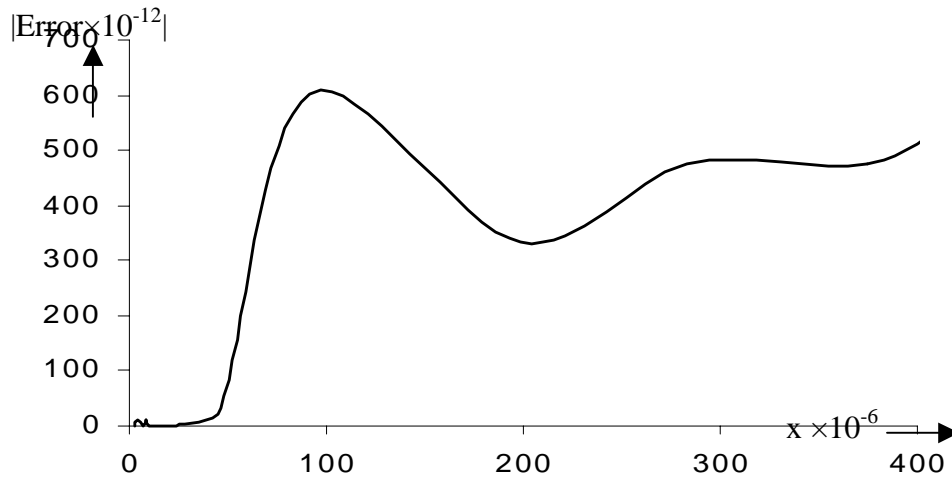


**Figure 5:** Magnitude of the error in the solution of the PDE  $u_t = (1/(\pi^2 - 1))u_{xx}$  obtained at time  $t = 0.9002$  using the transition matrix (DGHM multiwavelet with ap2 prefilter type) near the left boundary for the second multigrid with a grid size 1/16 of the actual size.

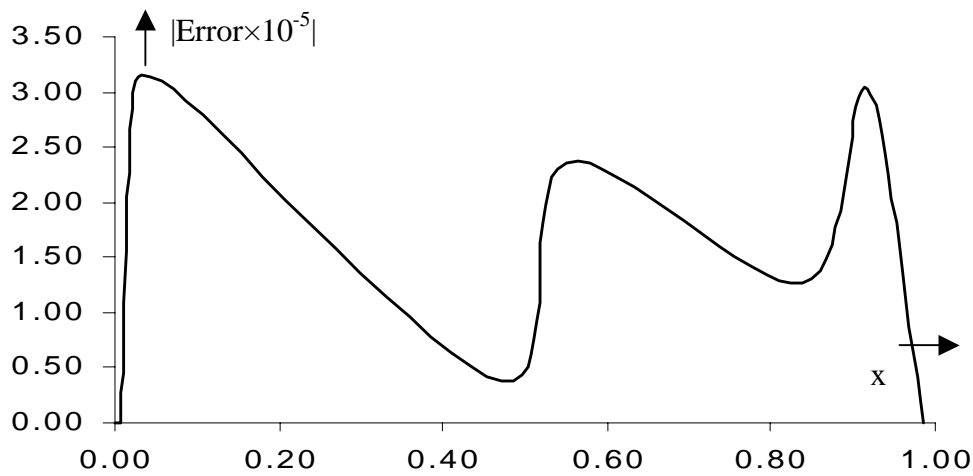


**Figure 6:** Magnitude of the error in the solution of the PDE  $u_t = (1/(\pi^2 - 1))u_{xx}$  obtained at time  $t = 0.9002$  using the transition matrix (DGHM multiwavelet with ap2 prefilter type) after a two-step multigrid correction near both left and right boundaries.

## 5. Conclusion

We demonstrated a general method to compute transition matrices required to solve PDEs. The smooth multiwavelet bases give less error compared to scalar wavelets and Legendre-type multiwavelets. The method proposed improves the error by 2 orders of

magnitude, for the same computational requirement when smooth multiwavelets are employed. The error near the boundary can be made smaller than that in the interior points by the new approach of introducing multigrids near the boundary alone. The method can be extended to 2-dimensional and 3-dimensional cases also.

## References

- [1] George W Pan. Wavelets in Electromagnetics and Device Modeling, Wiley-IEEE Press, Wiley series in Microwave and Optical Engineering, 2003.
- [2] G.Beylkin and J.M.Keiser. On the adaptive numerical solution of nonlinear partial differential equations in the wavelet bases .J.Comp.Physics.,132:233-259,1997.PAM report 262,1995.
- [3] B.Alpert, G.Beylkin, D.Gines and L.Vozovoi, Adaptive solution of partial differential equations in multiwavelet bases, J.Comput.Phys., 182(2002).
- [4] A.Averbuch, E.Braverman and M.Israeli, Parallel adaptive solution of a Poisson equation with multiwavelets, SIAM J.Comput., 22(2000).
- [5] A.Averbuch, M.Israeli and L.Vozovoi, Solution of time dependent diffusion equations with variable coefficients using multiwavelets, J.Comput. Phys. 150(1999).
- [6] Soltanian- Zadeh, Hamid, Jafari- Khouzani and Kouros, Multiwavelet grading of Prostrate pathological images, in Proc. SPIE vol.4684, P1130-1138, Medical imaging 2002: Image Processing, Milan Sonka; J.Micheal Fitzpatrick, May 2002.
- [7] G.Beylkin, RR Coifman and V.Rokhlin, Fast wavelet transform and numerical algorithms. J.Comm. Pure Appl. Math. 44.141-183, 1991.
- [8] G.Beylkin, J.M.Keiser and L.Volzovoi, A new class of stable time discretization schemes for the solution of nonlinear PDEs. J. Comp Physics 147:132-137, 1998.
- [9] Y.Capdeboscq and M.S. Vogelius, Wavelet based homogenization of a 2 dimensional elliptic problem, Hal-00021467, Version1, Mardi 21 Mars, 2006.
- [10] J.P.Geronimo, D.P.Hardin and P.R.Massopust, Fractal functions and wavelet expansion based on several functions, J. Approx Theory .Vol 78, pp373-401-September 1994.
- [11] D.P.Hardin and D.W.Roach, Multiwavelets prefilters I: orthogonal prefilters preserving approximation order  $p \leq 2$ , IEEE Trans Circuits Systems II. Analog Digital Process., 45(1998) pp1106-1112.
- [12] Fritz Keinert, Wavelets and Multiwavelets- Chapman & Hall/CRC Press, Dec 2003, ISBN 1-58488-304-9.
- [13] K.Attakitmongcol, D.P.Hardin and D.M.Wilkes, Multiwavelet prefilters II: Optimal orthogonal prefilters, IEEE Transactions. Image Processing, Volume10, Issue10, October 2001.
- [14] M.J.Vrhel and A.Aldroubi, Prefiltering for the initialization of multiwavelet transform in IEEE Proc. Inf. Conf. Acoust. Speech, Signal Processing, vol 3(Munich), pp2033-2036 April 1997

- [15] J.Lebrun and M Vetterli, High order balanced multiwavelets in IEEE Proc. Int. Conf. Acoust., Speech, Signal Processing, (Seattle, WA), 1998
- [16] I.Daubechies, Ten lectures on wavelets, CBMS-NSF Series in Applied Mathematics, SIAM, 1992.
- [17] B.Alpert, A class of bases in  $L_2$  for the sparse representation of integral operators, SIAM J. Appl. Math. Anal 24(1):246-262, 1993.
- [18] Hirotugu Akaike, Block Toeplitz matrix inversion, SIAM J. Appl. Math. Vol 24No.2, 234-241, March1973.
- [19] F.Arandiga, V.F.Candela and R.Donat, Fast multiresolution algorithms for solving linear equations: A comparative study, SIAM J. Sci. Comput., 16(1995)